Environmental Toxicology and Chemistry—Volume 37, Number 10—pp. 2619–2632, 2018
Received: 16 February 2018 | Revised: 26 March 2018 | Accepted: 2 July 2018

Environmental Toxicology

Rhizosphere Interactions Between Copper Oxide Nanoparticles and Wheat Root Exudates in a Sand Matrix: Influences on Copper Bioavailability and Uptake

Paul McManus,[a] Joshua Hortin,[a] Anne J. Anderson,[b] Astrid R. Jacobson,[c] David W. Britt,[b] Joseph Stewart,[a] and Joan E. McLean[a,*]

[a]Utah Water Research Laboratory, Civil and Environmental Engineering, Utah State University, Logan, Utah, USA
[b]Department of Biological Engineering, Utah State University, Logan, Utah, USA
[c]Department of Plants, Soils and Climate, Utah State University, Logan, Utah, USA

Abstract: The impact of copper oxide nanoparticles (CuONPs) on crop production is dependent on the biogeochemistry of Cu in the rooting zone of the plant. The present study addressed the metabolites in wheat root exudates that increased dissolution of CuONPs and whether solubility correlated with Cu uptake into the plant. Bread wheat (*Triticum aestivum* cv. Dolores) was grown for 10 d with 0 to 300 mg Cu/kg as CuONPs in sand, a matrix deficient in Fe, Zn, Mn, and Cu for optimum plant growth. Increased NP doses enhanced root exudation, including the Cu-complexing phytosiderophore, 2′-deoxymugineic acid (DMA), and corresponded to greater dissolution of the CuONPs. Toxicity, observed as reduced root elongation, was attributable to a combination of CuONPs and dissolved Cu complexes. Geochemical modeling predicted that the majority of the solution phase Cu was complexed with citrate at low dosing or DMA at higher dosing. Altered biogeochemistry within the rhizosphere correlated with bio-responses via exudate type, quantity, and metal uptake. Exposure of wheat to CuONPs led to dose-dependent decreases in Fe, Ca, Mg, Mn, and K in roots and shoots. The present study is relevant to growth of a commercially important crop, wheat, in the presence of CuONPs as a fertilizer, fungicide, or pollutant. *Environ Toxicol Chem* 2018;37:2619–2632. © 2018 SETAC

Keywords: Copper oxide nanoparticles; Copper toxicity; Root exudates; Wheat; Complexation; Deoxymugineic acid

INTRODUCTION

Copper oxide nanoparticles (CuONPs) are globally produced (Keller et al. 2013) for industrial applications in sensors, catalysts, solar energy conversion, electronic printing, surfactants, and antimicrobials (Bondarenko et al. 2012; Wang et al. 2013; Ahamed et al. 2013). They also have potential use in agriculture, as a nutrient source or as a pesticide (Monreal et al. 2015; Elmer and White 2016; Dimkpa and Bindraban 2017; Rodrigues et al. 2017). Application of these products in agriculture may contribute to their environmental accumulation. Incidental contamination of soils via waste streams and biosolid application may also occur (Lee et al. 2010; Rivera Gil et al. 2010). Copper oxide NPs are phytotoxic to lettuce and maize in hydroponic conditions with application of 10 mg NP/L (the lowest concentration tested; Wang et al. 2012; Trujillo-Reyes et al. 2014) and to beans in a sand matrix at the test concentration of 250 mg Cu/kg with no effect at 100 mg Cu/kg dosing (Dimkpa et al. 2015). Sublethal doses of CuONPs resulted in visible effects on root morphology, with shortening, fattening, and root hair changes at concentrations as low as 10 mg Cu/kg (Wright et al. 2016; Yang et al. 2018). When added to soil (loamy sand, 1.6% organic carbon, pH 6–6.5) CuONPs at 500 mg Cu/kg also showed toxicity via decreased root length in wheat (Gao et al. 2018) but had little effect on green peppers grown in a silty loam soil (pH 7.5; Rawat et al. 2018). Differences in soil properties (pH, organic matter content, mineral type and concentration), plant-dependent responses (rhizosphere processes including pH alterations and root exudates), and experimental designs influence CuONP bioavailability and, thus, test results. This necessitates an increased understanding of the responses induced in plants by NPs preceding further NP use in agriculture.

Copper is an essential micronutrient for plant growth. In general, plants regulate Cu concentrations in aboveground tissue at an upper threshold of 20 to 30 mg Cu/kg dry shoot mass

This article includes online-only Supplemental Data.
* Address correspondence to joan.mclean@usu.edu
Published online 5 July 2017 in Wiley Online Library (wileyonlinelibrary.com).
DOI: 10.1002/etc.4226

(Marschner 1995). The upper threshold for wheat is reported as 17 to 18 mg Cu/kg dry shoot weight (Davis and Beckett 1978; Fageria 2001). At levels above this threshold, Cu becomes toxic (Marschner 1995; Michaud et al. 2007, 2008). Plant mechanisms for maintaining homeostasis of Cu include producing specific metabolites in root exudates to increase or decrease bioavailability of Cu from the rhizosphere regulating Cu uptake. Metallochaperones move Cu internally, with sequestration as a nonharmful form (Clemens et al. 2002). Specific efflux pumps remove Cu from the cells (Clemens et al. 2002), and Cu binding to plant cell walls is seen in roots (Kopittke et al. 2011, 2014; Peng et al. 2015; Meychik et al. 2016). Phytotoxicity occurs when these systems are overwhelmed.

The bioavailability of Cu is controlled by soil-solution phase chemistry, particularly in the region surrounding the root surface, the rhizosphere. Porewater pH and dissolved organic carbon (DOC) are most influential on Cu mobility and bioavailability (Sauve et al. 2000; Michaud et al. 2007). Copper exists in solution in the rhizosphere as a free ion (Cu^{2+}) or as complexes with inorganic or organic ligands. The metabolites released from the roots in exudates and secreted from root-colonizing microbes complex Cu among other metals, driving soil Cu mineral dissolution and affecting bioavailability because ligands are differentially taken up by plants (Parker et al. 2001; Violante and Caporale 2015; Chen et al. 2017). These same processes that affect soil Cu mineral dissolution will also affect CuONP solubility. Uncertainty remains regarding the extent to which CuONPs may inflict toxicity directly or via Cu ions released from the CuONPs (Stampoulis et al. 2009; Shi et al. 2011; Atha et al. 2012; Trujillo-Reyes et al. 2014; Anjum et al. 2015), but increasing ion release via exudate dissolution of NPs will drive the bioavailability and toxicity of Cu.

Metabolites in wheat root exudates that complex Cu include the phytosiderophore 2′-deoxymugineic acid (DMA), which is secreted from wheat roots grown under Fe-deficient conditions and, in addition to forming Fe–DMA, will complex with Cu (Ma and Nomoto 1993; Xuan et al. 2006). The stability constant for the Cu–DMA complex ($\log K = 18.7$) is similar to that for Fe(III)–DMA ($\log K = 18.4$; Murakami et al. 1989). Indeed, the lower Fe levels in shoots of wheat grown in hydroponic solutions with increased dosing of Cu (Michaud et al. 2008) may be attributable to the phytosiderophore–Cu complexation limiting Fe uptake. Other low–molecular weight organic acids in root exudates, such as citrate and malate, also complex Fe and Cu, to solubilize minerals. Increased solubility through complexation can drive uptake into the plant or root-associated bacteria. For example, citrate complexes Cu and enhances Cu uptake by the root colonizer *Pseudomonas putida* (McLean et al. 2013). Amino acids also leach sufficiently high levels of Cu from CuONPs to cause toxicity to the bacterium *Escherichia coli* in culture solutions (Gunawan et al. 2011). Soil application of the root exudates oxalate and citrate from the leopard lily, *Belamcanda chinensis*, increase Cu uptake in a grass, *Echinochloa crus-galli* (Kim et al. 2010). Competing similar stabilities between Cu and Fe for various ligands makes this system in the rhizosphere nontrivial (Callahan et al. 2006). The concentrations of organic ligands in the root exudates, which play a crucial role in metal bioavailability in the rhizosphere, increase with higher doses of Cu ions (Nian et al. 2002; Michaud et al. 2008). Effects of CuONP doses on root exudation have implications for plant metal uptake and homeostasis (Clemens 2001), thus illustrating the need to understand solution phase biogeochemistry in the rhizosphere.

Hydroponic studies illustrate that Cu complexes may increase or decrease Cu bioavailability (Parker et al. 2001; Michaud et al. 2008; Ryan et al. 2013). However, hydroponic systems have several shortcomings. Jones (1998) highlights that hydroponically grown roots are morphologically and physiologically different from those grown in solid systems, including the lack of root hairs, mechanical impedance, and water stress. For example, hydroponic systems overestimated 50-fold the phytosiderophore release rates from wheat compared with plants grown on a calcareous soil (Oburger et al. 2014). Gao et al. (2018) in an agricultural soil emphasized the importance of rhizosphere factors such as pH alteration and exudation in influencing dissolution of CuONPs. However, no quantification of specific exudates was performed (Gao et al. 2018).

The present study evaluates the interactions between root exudates of bread wheat (*Triticum aestivum* cv Deloris) and CuONPs at sublethal levels in a sand matrix. This model solid matrix acts as a proxy for soil in terms of plant root morphology, mechanical impedance, and water stress, while allowing for the isolation of root exudates and determination of Cu–exudate complexes. Plants grown in sand lack contributions from dissolved organic compounds typically found in soils, such as fulvic acids or metabolites from the soil microbes, that could act as metal ligands. This allows for a focus on the evaluation of ligands produced by the plant in response to CuONP challenges. Indeed, the restricted low Fe content of sand promotes the secretion of phytosiderophores that likely participate in dissolution of the NPs and complexation of Cu. Our findings will demonstrate the rhizosphere processes that influence the role of plant exudates in the responses of plants to growth with CuONPs. Specifically, the present study addresses how root exudate metabolites drive dissolution of the NP into Cu^{2+} ions and complexes to affect Cu uptake by the wheat plant. Although other research suggests that root exudates function in the dissolution of NPs in the rhizosphere (Peng et al. 2017; Gao et al. 2018), the process has not been fully studied. In the present study, the solution phase of the wheat rhizosphere was analyzed to better understand CuONP–wheat root interplay. From the findings, mechanisms of CuONP toxicity were inferred, and the plant response in managing metal homeostasis was investigated.

MATERIALS AND METHODS

Characterization of NPs

Copper oxide NPs obtained from Sigma-Aldrich (product no. 544868), nominal manufacturer reported size <50 nm, were characterized in deionized water and in porewater from wheat-planted sand for aggregation, shape evolution, and surface charge (Dimkpa et al. 2011, 2012, 2013; Supplemental Data, Table S1). Characterization showed that the CuONPs

aggregated to submicron-sized clusters in both deionized water and the presence of wheat plants (Dimkpa et al. 2011, 2012, 2013). The CuONPs contained low levels of Al, Fe, Mn, and Zn contamination (<0.02% metal/kg NP; Hortin 2017).

Plant growth conditions

White silica sand (UNIMIN) was washed with deionized water 3 times and heated for 12 h in a 550 °C muffle furnace to remove organic matter. After washing in deionized water again, sand was dried at 150 °C. Some soluble organic matter remained despite the muffle furnace treatment. The background DOC was <5 mg/L in a 2:1 water:sand extraction, and 1.5 mg/L each of formate, acetate, and gluconate were detected.

Nitric acid digestion of the muffle furnace–treated sand showed low amounts of total Al (746 mg/kg), total Fe (347 mg/kg), and total Cu (0.4 mg/kg); <2% of these levels were water-soluble (2:1 deionized water:sand; Supplemental Data, Table S2). A diethylene triamine pentaacetic acid (DTPA)–ammonium bicarbonate extraction (Reed and Martens 1996) was performed to assess plant available metals in the sand. Use of DTPA (0.005 M) buffered with ammonium bicarbonate extraction at pH 7.6 is a standard test to define nutrient requirements in alkaline soils for various crops, including wheat (Reed and Martens 1996). The sand was deficient in Fe, Zn, Mn, and Cu for optimum wheat growth (Supplemental Data, Table S2). Water content at field capacity of the sand was determined by allowing the saturated sand to freely drain overnight, and the results (10% m/m) were similar to those reported by Saxton and Rawls (2006).

Growth studies were established in a randomized block design with studies being blocked on time, because of limitations in handling and analyzing the number of growth pots at harvesting. Each experimental design was repeated 3 times, with triplicate replications of treatments within each study time. The studies were replicated completely, as opposed to one CuONP dose each time, to avoid biological and procedural bias. The first 2 experimental replicate sets included a control (no NPs) and dosing at 30, 100, and 300 mg Cu/kg. The third experimental replicate included 2 additional doses of CuONPs (10 and 200 mg Cu/kg). The dose range was selected to include levels that, although sublethal, caused a significant decrease in root length correlating with increased oxidative stress (Dimkpa et al. 2012).

The CuONP powder was added to dry sand at the specified doses, followed by shaking the mixtures for 30 min in acid-washed 1000 mL HDPE Nalgene bottles to homogenize the samples. The sand–NP samples were autoclaved and distributed into sterile Magenta™ growth boxes (21 × 7 × 7 cm; Sigma-Aldrich) used for planting. Autoclaving would not have affected this already oxidized, crystalline CuONP. A $Ca(NO_3)_2$ filter-sterilized solution (0.7 mM) was added to the sand in the Magenta boxes for wetting the sand and providing background ionic strength, with Ca promoting seed germination and root growth.

In preliminary studies, 300 g of sand was used for plant growth at all concentrations of CuONPs. With the lower CuONP doses, the roots extended through the sand to the box base; but at the higher dosing, stunted roots penetrated only the top 2 cm of the sand. To ensure that the roots were fully distributed throughout the sand for all treatments (i.e., so that all of the sand and CuONPs are rhizosphere-influenced), the mass of sand was reduced proportionally (Supplemental Data, Table S3). The 0.7 mM $Ca(NO_3)_2$ solution was added to the previously homogenized NP–sand mixture at 1.5 times the water content at field capacity (a solution to sand ratio of 0.15 mL/g). The Magenta boxes are completely enclosed, so there was no free drainage of the added solution and minimal loss as a result of evapotranspiration.

Seeds were surface-sterilized by immersing in 3% NaOCl (Clorox) for 10 min, followed by rinsing in sterile deionized water, and pregerminated on lysogeny broth agar plates for 4 d, to assess microbial sterility. Microbe-free seedlings (25 per Magenta box) were transferred to the treated sand. Plants were grown for 10 d (14 d postgermination) under fluorescent lights (28 °C, 16:8-h light:dark, generating a photosynthetic photon flux density of 144 $\mu mol\, m^{-2}\, s^{-1}$ at the lid of the Magenta box) in conditions previously described (Dimkpa et al. 2012, 2013). Boxes having a higher CuO NP dose and less sand were raised such that the level of the sand relative to the incident light was uniform for all treatments. Boxes were randomly moved daily to minimize any light effects on the shoots. Boxes containing equivalent NP treatments without plants, termed "unplanted," were included as abiotic controls. Treatments using a Cu salt, as a Cu ion control, were not included. Addition of a Cu salt at concentrations based on measurements of CuONP solubility in the sand matrix (Dimkpa et al. 2012) do not mimic the dynamic uptake/dissolution process of the NP-planted system; Cu ion release from NPs in wheat-planted systems is time-dependent and generates an intense gradient from the NP source (Dimkpa et al. 2012).

Analysis of plant tissues and sand after harvesting

At harvest, the roots were distributed throughout the sand growth matrix (Supplemental Data, Figure S1); the root directly influenced the sand–NP mixture. After 10 d of growth in contact with the NPs (14 d postgermination), 0.7 mM $Ca(NO_3)_2$ solution was added to each box with the seedlings to flush exudates from roots. This process was started 3 h after the start of the photoperiod for maximum phytosiderophore exudation (Oburger et al. 2014). The volume used for each treatment was equivalent to the volume added at seed planting (Supplemental Data, Table S3). An exception was for the 300 mg Cu/kg dose, where an additional known volume was added (Supplemental Data, Table S3) to provide adequate volumes for analyses. The solution was equilibrated with the sand in the presence of the plants for 15 min. Plants were removed from the sand and measured for longest root and shoot, and roots were washed thoroughly with deionized water. Shoots were cut above the coleoptile because our observations indicate that CuONPs are bound to this tissue, biasing shoot uptake results (Wright et al. 2016). Tissue was dried overnight at 60 °C, digested using nitric

acid (Jones and Case 1990), and analyzed for Cu, Fe, Mn, Ca, Mg, and K by inductively coupled plasma mass spectroscopy (ICP-MS; Agilent 7700x; US Environmental Protection Agency 1986 [method 6030]). The sand from each box was thoroughly mixed and extracted using nitric acid and hydrogen peroxide (US Environmental Protection Agency 1986 [method 3050]) with analyses of the extract for trace elements and major cations by ICP-MS.

Analysis of porewater

Porewater was removed from sand by transferring the contents of the boxes into autoclaved, 100-mm diameter, long stem glass funnels stopped with glass wool and placed onto vacuum flasks. Extraction of the liquid from the sand was aided with application of a vacuum. The collected solution was then filtered through a 0.2-μm nylon filter (Environmental Express) to remove aggregated NPs and large composites from plant growth. The intent of the present study was to evaluate the chemistry of dissolved Cu.

To evaluate metal speciation in greater detail than traditional methods, the "soluble" fractions were differentiated by size using 2 methods, microcentrifugation and 3-kDa ultrafiltration. In water quality analysis "dissolved" has been traditionally defined as the filtrate collected after passage through a 0.45- or, more recently, a 0.2-μm filter. Because NPs are defined as particles <100 nm in at least one dimension, intact or partially dissolved nano-sized particles, but not their aggregates, will pass through a 0.2-μm filter (Gajjar et al. 2009; Dimkpa et al. 2012, 2013). Thus, from traditional environmental science definitions, NPs would normally be classified as "dissolved"; but in the context of nanotoxicology, further distinctions are important because the size of the particle has direct implications for bioavailability and toxicity (Mudunkotuwa et al. 2012). The NPs must be removed to accurately define dissolved Cu. To better define dissolved Cu, porewaters were centrifuged at 14 000 *g* for 14 min using an Eppendorf centrifuge 8504 (Eppendorf rotor F45-30-11; Dimkpa et al. 2012, 2013) before ICP-MS analyses. Based on the Stokes-Einstein equation, this procedure sedimented particles >30 nm. Dynamic light scattering (DLS; DynaPro NanoStar; Wyatt Technology) showed that the remaining particles in solution after centrifugation had a mean diameter of 8 nm. Aggregation of CuONPs previously observed in deionized water and sand matrices (Dimkpa et al. 2012, 2013) may explain the lack of particles in the 10- to 30-nm range; therefore, this fraction of Cu is defined in the present study as $Cu_{<10.}$ This fraction could include Cu^{2+}, Cu complexed to ligands <10 nm, and Cu associated with suspended material <10 nm including NPs. To remove NPs <10 nm, additional solutions were processed through 3-kDa Amicon-Ultra Centrifugal Ultrafilters (Millipore; 4000 *g* for 30 min), estimated to remove CuONPs >2 nm ($Cu_{<2}$) based on pore size analysis (Guo and Santschi 2007). This fraction includes Cu^{2+} and Cu complexed to ligands <2 nm. Subsequent DLS analysis of the filtrate confirmed removal of all particles >2 nm. Free Cu^{2+} activity was measured using a Cu ion-selective electrode (Orion 96-29 Ionplus) following the procedures described by Rachou et al. (2007) for solutions with low ionic strength and DOC. The electrode was calibrated against a solution of 1 mM iminodiacetic acid, 1 mM Cu-nitrate, 6 mM NaOH, and 2.5 mM K acid phthalate. By altering the pH, the extent of Cu complexation varied in solution to provide free Cu^{2+} for probe calibration from 10^{-4} to 10^{-14} M.

The pH of the 0.2-μm filtered solution was determined by standard methods (American Public Health Association 2012 [method 4500]). Dissolved organic carbon was determined for both the microcentrifuged supernatants, defining the <10 nm fraction ($DOC_{<10}$), and the 3-kDa ultrafilter filtrates, defining the <2 nm fraction ($DOC_{<2}$), by combustion using a TOC analyzer with IR detection (Apollo 9000; Teledyne Tekmar; method 5310 B [American Public Health Association 2012]). Amino acids in the 0.2-μm filtered solution were determined by high-pressure liquid chromatography (HPLC; Aquity; Creager et al. 2010). Ion chromatography using a Dionex ICS-3000 equipped with a Dionex IonPac AS11-HC analytical column and guard column and a Dionex ASRS-ULTRA Anion Self-Regenerating Suppressor (Dionex) determined low–molecular weight organic acids. For total carbohydrates, a sulfuric acid method with a glucose standard was used, with quantification using a Genesys 6 ultraviolet-visible spectrophotometer (Thermo Scientific) at 315 nm, per Albalasmeh et al. (2013). Protein concentration was determined via the BCA Protein Assay Kit (Thermo Scientific) measuring absorbance at 576 nm. Acetone precipitation was used to minimize interferences.

The phytosiderophore DMA was determined in the 3-kDa ultrafiltrate (Millipore) and quantified against a certified standard (Toronto Research Chemical) by liquid chromatography triple quadrupole mass spectroscopy (LC-QqQ-MS; Agilent 1290 ultra HPLC 6490) with a zwitterionic column (150 × 1.0 mm i.d.) and a guard column (14 × 1.0 mm i.d.) from SeQuant. The LC-QqQ-MS was operated using dynamic multiple reaction monitoring mode with chromatograms for the 305 to 186 transitions for quantifying DMA. The mobile phase was 0.1% formic acid, similar to the method described by Schindlegger et al. (2014). The 3-kDa microcentrifuged filtrate was analyzed because the <10 nm fraction led to carryover of Cu during analysis. The molecular weight of DMA is 304.299 g/mol, and DMA is a sexadentate-chelating agent, forming a 1:1 complex with Cu^{2+} and 1:1 complexes with Fe^{3+}, with or without inclusion of H^+ or OH^- (Murakami et al. 1989). These complexes would pass a 3-kDa filter. The samples also were acidified to release Cu or Fe from the complex to measure total uncomplexed DMA.

Data processing

Maintaining a uniform density of the rooting system throughout the sand for each dosing of NPs required a reduction in the amount of sand used at the higher CuONP concentrations because of NP-stunted root morphology. Volumes of the 0.7 mM $Ca(NO_3)_2$ solution applied to the sand at planting and for extraction were also proportionally varied for each treatment (Supplemental Data, Table S3). Water loss during growth was assessed in a separate experiment, with identical conditions as above. After 10 d of growth, plants were removed carefully; the

remaining sand was mixed thoroughly before removing triplicate samples from each Magenta box and drying at 60 °C. The percentage moisture was used to assess how much water remained in the sand. The same was done for unplanted replicates. Because each treatment used a different volume of $Ca(NO_3)_2$ for planting and extraction and the treatment affected water uptake by plants, volumes were normalized to the volume of water in the sand after harvesting. This factor was applied to all concentrations (metals and ligands) to account for dilution by extraction volume.

Statistical analysis

We used JMP 8 (SAS Institute, Ver 5.01) for one-way analysis of variance (ANOVA) blocked on 3 experiments repeated over time and Tukey's honestly significant difference to compare significant responses from different NP doses. Transformations (log) were performed to satisfy constant variance and normality when required. Power of the test was also calculated at >75% with $n = 9$. Data below method detection limit, the censored data, were imputed using a log-normal distribution of quantifiable data and assigned a value randomly based on an extrapolation of that log-normal distribution (Cohen 1959). This method was only applied if >60% of the data were reportable to define the distribution of quantifiable values. This method removed bias from censored data and was only necessary for parameters in control treatments (no plant or CuONPs). Principal component analysis was used to explore relationships between plant response and solution characteristics, including concentration of Cu^{2+}, Cu ligands, pH, and DOC. Pearson's correlation coefficients (R) were also generated to confirm relationships between variables.

Geochemical modeling

Copper complexes were modeled in the truly dissolved fraction of the porewater (<2-nm fraction) using MINTEQ (Gustafsson 2014). Model inputs (Supplemental Data, Table S4) included the ligands determined from chromatography in the porewater, the concentration of soluble metals defined as $M_{<2}$ quantified by ICP-MS in the filtrate from spin-filters, and pH. Stability constants for Cu and Fe complexation with DMA (Murakami et al. 1989), gluconate (Gajda et al. 1998; Bechtold et al. 2002), and amino acids from GEOCHEM (Parker et al. 1995) were added to the model's database. The model was run with precipitation allowed (indicating equilibrium). The CuONPs were modeled with a finite type IV solid phase of crystalline tenorite, calculated as total mass of CuONPs added initially to the Magenta boxes per volume of solution at the end of the growth period. X-ray diffraction analysis of the CuONPs showed the patterns typical for a monoclinic structure of tenorite (Stewart et al. 2015). Currently, the stability constant for nanoparticulate tenorite is not reported in the literature. David et al. (2012) determined for ZnO that the log K_{sp} values for bulk and larger NPs (20 and 71 nm) were not different. The only stability constant that differed from bulk was for the 6-nm ZnO NPs. The present modeling effort serves as a first approximation of CuONP–solution phase interactions.

Quality control

Solution samples without filtration and one root from each box were plated on lysogeny broth medium to assess microbial colonization at plant harvest. Overall, 75% of plant roots and solution plated onto lysogeny broth showed no culturable bacterial or fungal infection after 5 d of plating. After 10 d, growth of microbes presumed to be dormant bacterial endophytes was evident in some root samples.

All treatments were replicated in triplicate within each experimental setup. For NP dosing at 0, 30, 100, and 300 mg Cu/kg, the experimental setup was repeated 3 times over a 3-mo period to account for biological variability (triplicate within experiment times 3 experimental setups, $n = 3 \times 3 = 9$). For dosing at 10 and 200 mg Cu/kg the experimental setup was performed once with each treatment in triplicate ($n = 3$). This was done for both planted and unplanted Magenta boxes. Unplanted controls were used to show CuO dissolution in 0.7 mM $Ca(NO_3)_2$ matrix and to ensure that DOC was derived from biological exudates. Controls of plants without NP addition were also included to observe plant growth and Cu uptake associated with Cu present in the seed. The US Environmental Protection Agency's quality control protocols for ensuring accuracy and precision were followed for all analyses, including the use of blanks, calibration check samples, replicate analyses, and matrix spike samples.

RESULTS AND DISCUSSION

Plants responded with changed metal uptake and morphology

Dose-dependent reduction in root elongation was observed with wheat growth in the CuONP-amended sand (Figure 1A), as reported (Dimkpa et al. 2012, 2013). Root dry mass decreased by 50% for the dose of 300 mg Cu/kg sand compared to the control (Figure 1B). Shoot length and dry weight, however, were not affected by NP dose (15.65 ± 1.44 cm, averaged shoot length; 0.185 ± 0.024 g, shoot dry weight). Minimal chlorosis (1–2 leaves out of 50 leaves per box and only slight yellowing) was found at the end of the 10-d growth period, even in the control with no NPs and, thus, was not caused by exposure to the CuONPs but rather the depletion of nutrients stored in the seed.

Fageria (2001) and Davis and Beckett (1978) suggested an upper threshold of 18 mg Cu/kg dry shoot mass for wheat to provide this essential nutrient without a decrease in yield, with deficiency suggested below 1 to 5 mg Cu/kg dry shoot. In the present study, with 10-d-old plants, the background Cu level (no added NPs) was approximately 20 mg Cu/kg dry shoot (Figure 1C), coming from supplies stored in the seed. Copper increased up to 50 mg Cu/kg dry shoot when grown with doses of CuONPs of 100 mg Cu/kg sand and above, yet there was no effect on shoot length or shoot dry weight (Figure 1C). Copper

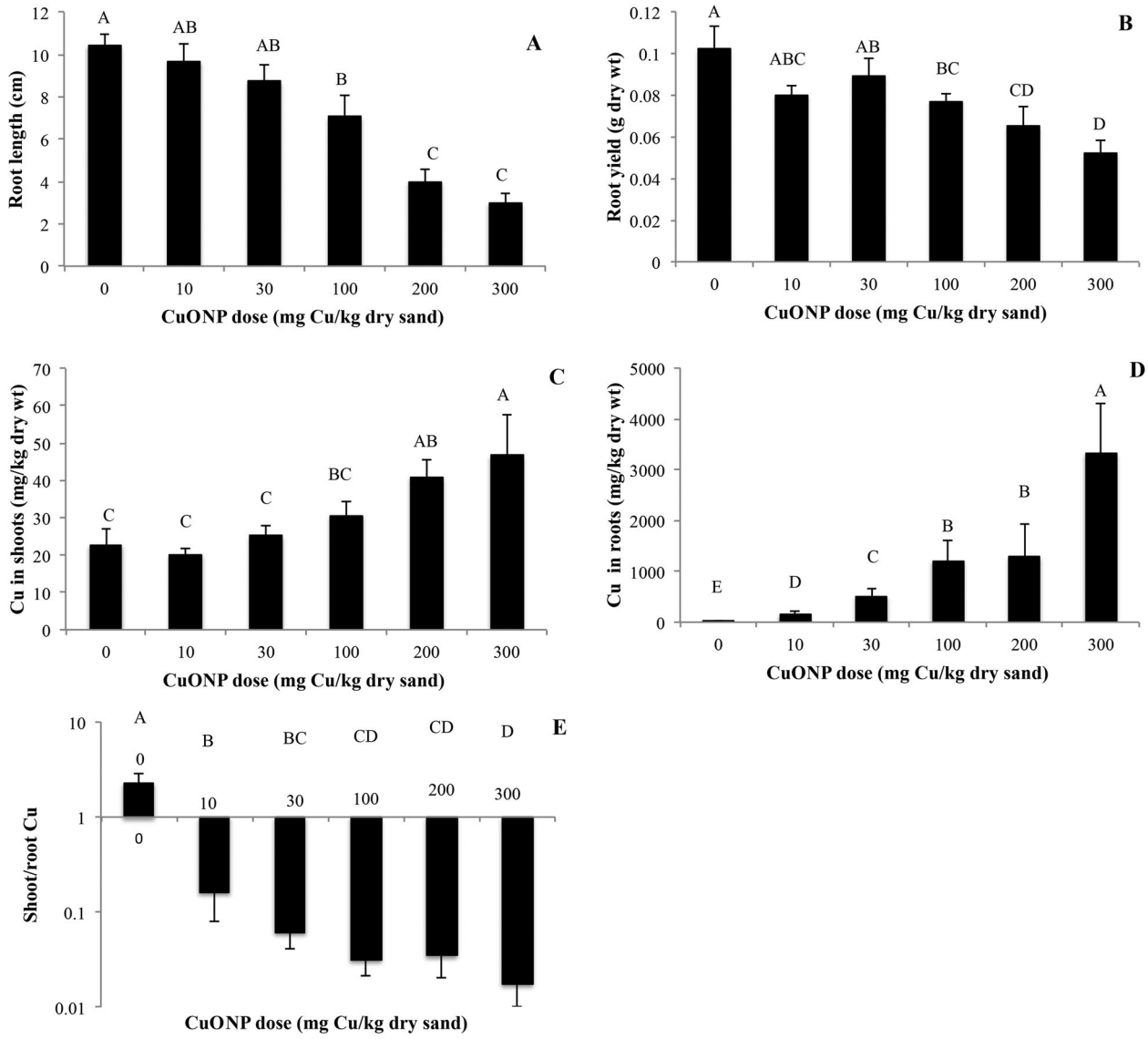

FIGURE 1: Response of wheat plants at 10 d of growth to dosing with copper oxide nanoparticles (CuONPs) as expressed by root length (**A**), root dry weight yield (**B**), Cu concentration associated with the roots (**C**), Cu concentration in shoots (**D**), and the Cu concentration ratio in shoot/root (**E**). Treatments with the same letters are not significantly different ($\alpha = 0.05$) by Tukey's honestly significant difference after log transformation. Error bars are 95% confidence interval to illustrate the spread in the data.

homeostasis in shoots was not maintained with doses of 100 mg Cu/kg sand and above, concentrations that changed root morphology.

Root-associated Cu increased dose-dependently (Figure 1D), with these values including both surface-adhered particles and Cu inside the tissues. The roots assayed had been rinsed only with deionized water, to avoid tissue damage and leakage occurring with more rigorous cleaning methods. Despite not distinguishing between Cu physically associated with the roots, such as agglomerates on root hairs (Adams et al. 2017) and within root cells, the concentration of Cu associated with the roots was orders of magnitude higher than in the shoots, implying control of translocation of Cu within the plant, as reported by Gao et al. (2018) for wheat and in rice (Peng et al. 2015, 2017). In the present study, only the control showed greater accumulation of Cu in the shoots than roots, with a shoot to root ratio >1; all doses of CuONPs resulted in partial exclusion of Cu partitioned into shoots (shoot/root >1; Figure 1E).

Transport of Cu^{2+} within a normally functioning plant is tightly controlled by ligand exchange reactions within the plant. Copper is sequestered in vacuoles of the root cells (Clemens et al. 2002) as an exclusion strategy (Baker 1981). The observed binding of Cu to root cell walls also would limit Cu flux to the shoots (Kopittke et al. 2011, 2014; Peng et al. 2015; Meychik et al. 2016). The translocation of intact CuONPs with subsequent dissolution of CuONPs in planta also, however, is a potential mechanism for increased uptake into the shoot (Wang et al. 2012). In the present study, concentrations >100 mg Cu/kg sand had increased shoot Cu uptake compared to control plants (Figure 1D). The form of the Cu loaded into the shoots was not determined. Damage to a cell's plasmalemma function by

CuONPs and/or Cu ion (Lee et al. 2008) could promote ingress and flux of NPs along with Cu^{2+} ion or Cu complexes through the plant to the shoots. Dimkpa et al. (2013, 2012), using X-ray absorption spectroscopy, identified Cu complexes in wheat shoots. The shoot tissues had decreased chlorophyll contents and increased oxidative stress in the roots, as determined by increased lipid peroxidation and oxidized glutathione (Dimkpa et al. 2012). Molecular analysis confirmed increased expression for genes functioning in Cu chelation (Wright et al. 2016; Yang et al. 2018) as examples for activated mechanisms for tolerance to Cu, such as limiting Cu translocation into shoot tissue (Figure 1E).

Increasing NP dose corresponds with increasing DOC exudation

Dosing with increasing concentration of CuONPs, whether a direct effect of the NPs or released ions, resulted in an increase in wheat root exudation measured as changes in the DOC in the porewaters (Figure 2A). Changes in DOC were not observed in the unplanted, abiotic controls (31.6 ± 12.3 mg C/L; average ± 95% confidence interval). There were no differences in DOC concentration in the planted system in the porewaters dependent on the processing methods of filtration versus centrifugation (i.e., 2-μm filter vs 10 nm centrifugation and 2 nm spin-filter). Thus, all DOC arising from root exudates, including low–molecular weight organic acids, phytosiderophores such as DMA, amino acids, and sugars, were molecules <2 nm in size.

The concentration of Cu in the porewater was dose-dependent (Figure 2B); however, only 56% of Cu in the porewater was defined as dissolved (<2 nm in size). The remaining fractions were CuONPs >2 and <10 nm that may be a product of NP remodeling during incubation in the planted sand because there was no difference in Cu concentration with size for the unplanted control. Because the DOC was all <2 nm, Cu in the >2 and <10 nm fraction was not associated with organic colloids. Dissolved Cu (defined as $Cu_{<2}$) accounted for <0.1% of the added Cu in the NPs (Figure 2C).

The pH of the porewater at the end of the growth period was influenced by CuONP dose. The pH was higher with growth at 200 and 300 mg Cu/kg (ANOVA $p < 0.0001$; pH 7.5 ± 0.3) compared with a pH of 6.7 ± 0.1 from growth with doses of 0, 10, and 30 mg/kg (Supplemental Data, Table S5). The change in pH with dosing can be, in part, connected with the proton-consuming reaction for the dissolution of CuO (e.g., $CuO + 2H^+ = Cu^{2+} + H_2O$), although the extent of pH change is mitigated by the buffering capacity of the system. Plants also respond to metal challenges by altering the pH of the rhizosphere. Gao et al. (2018) reported a half of a unit increase

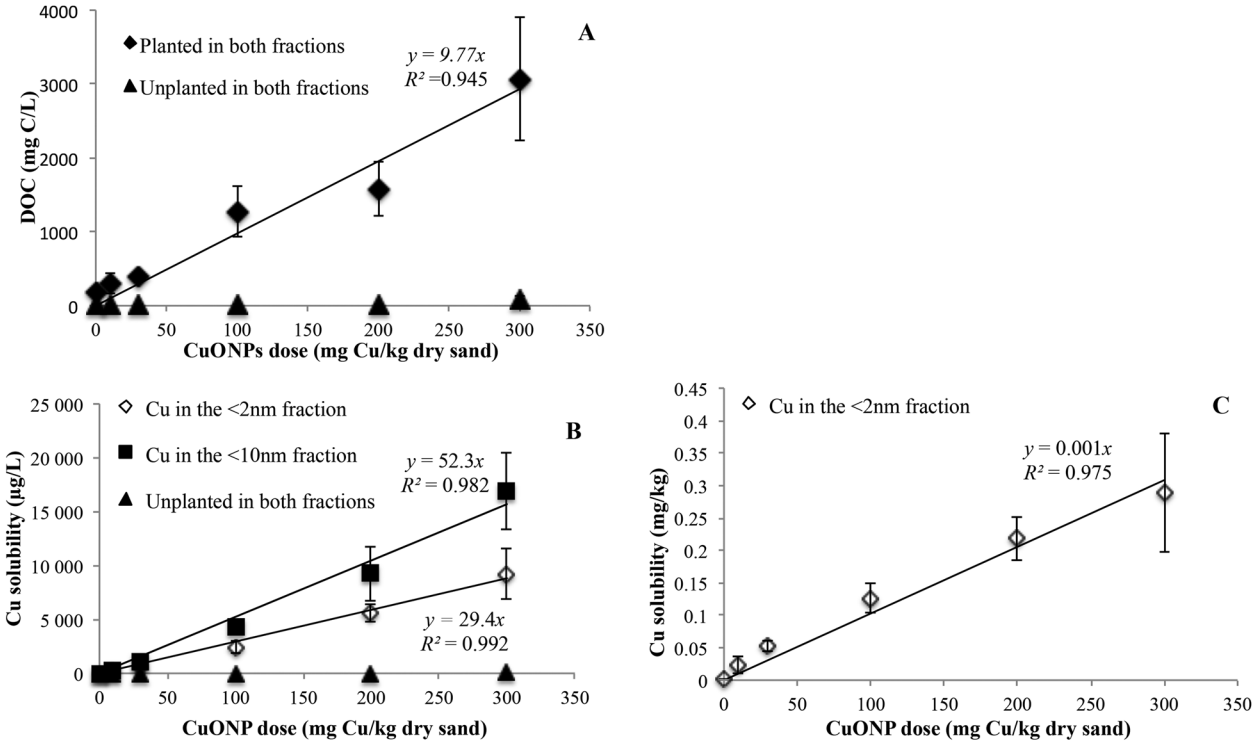

FIGURE 2: Dissolved organic carbon (DOC) and copper (Cu) porewater concentrations at 10 d of wheat growth dosed with Cu oxide nanoparticles (CuONPs). Concentration of DOC in porewater (there was no difference in DOC concentration in the fractions of filtration size, <10 and <2 nm; all DOC is <2 nm in size or <3 kDa), (**A**). Copper in porewater distinguished by filtration size, as $Cu_{<10}$ and $Cu_{<2}$, across doses of CuONP in planted and unplanted systems (**B**). For the unplanted, there was no difference in concentration with filter size. Dissolved Cu ($Cu_{<2}$), now expressed as milligrams per kilogram in the planted system, accounted for <0.1% of the added Cu in the nanoparticles (**C**). Free Cu^{2+} concentration in the porewater from the planted system ranged from 0.32 to 3.6 μg/L. Error bars are 95% confidence interval to illustrate the spread in the data.

in pH (pH 6 to 6.5) of a wheat rhizosphere soil exposed to 500 mg Cu/kg as CuONPs compared to the bulk soil, which they attributed to a plant response to exposure to Cu ions. A pH effect with dosing was not observed in the unplanted system (pH 7.71 ± 0.37) because <30 μg Cu/L was solubilized. There was higher variability in pH in unplanted systems attributable to low salt content and poor buffering, resulting in no statistical difference (paired t test) between plant and unplanted systems at each dosing.

The solubility of CuO as tenorite decreases an order of magnitude with every 0.5 pH unit increase (Lindsay 1979), so the enhanced dissolution with increasing pH is counter to theory. The increased DOC released from the roots enhanced the chelation power of the porewater, promoting CuO dissolution such that it compensated for the decreased solubility with rise in pH.

In the porewater, DOC and soluble $Cu_{<2}$ were correlated ($r = 0.976$, $p < 0.0001$; Figure 2A and B), supporting the hypothesis that biological exudates drove NP dissolution. In the unplanted system (i.e., sand amended with NPs but not planted), the porewater had only background-detectable DOC (Figure 2A) and the maximum concentration of $Cu_{<2}$ in solution was 28 μg/L with up to 88% of the $Cu_{<2}$ was as the free ion Cu^{2+}. Porewater from planted systems, with higher DOC, showed a lower ratio of $Cu^{2+}/Cu_{<2}$ compared to unplanted treatments because free Cu^{2+} was assessed at 1% of $Cu_{<2}$. Thus, the complexation engineered by the metabolites in the DOC was a major driving force in CuONP dissolution in the planted systems.

Growth of wheat with CuONPs increased soluble Cu from the NPs in the porewater because of complexation of Cu with ligands in the root exudates, thus subjecting the plants to Cu toxicity. These processes constitute a feed-forward response with NP exposure (i.e., with increasing NPs and associated soluble Cu, more DOC is released, driving NP dissolution), having positive implications for properly dosed nano-fertilizers but potentially less favorable outcomes for higher doses/contamination. Reduced root lengths (Figure 1A) may be offset by a proliferation of longer root hairs, which is observed in wheat grown with CuONPs (Adams et al. 2017); these morphological changes could alter exudate release. Studies of root morphology and exudate status over time may shed light on this process.

Increasing exudation drove dissolution of CuONPs

The characterized low–molecular weight organic acids, amino acids, and DMA combined contributed 15 ± 5% to the DOC in the root exudates. The remaining carbon was present as carbohydrates (70 ± 30%) and proteins (15 ± 13%). The neutral carbohydrates (e.g., sucrose, glucose, fructose) in the root exudates are expected to play minor roles in dissolution of Cu from the CuONPs because they lack carboxylic, S- or N-based functional groups involved in Cu complexation. They were shown not to drive dissolution of CuONPs in supporting information by Wang et al. (2013). However, it is possible that certain larger carbohydrates may bind and cap the CuONPs, though no literature has currently been found to qualify this. Proteins, however, can form surface "coronas" on NPs (Lynch and Dawson 2008; Xu et al. 2012), impacting the bioavailability and bioreactivity of the NPs. For example, specific peptides adsorb to CuONPs (Joshi et al. 2012), potentially altering the CuONP bioreactivity.

Porewaters from unplanted sand had no citrate, malate, or DMA and 70% lower gluconate compared to the respective planted CuONP dose, indicating that DOC compounds were plant-associated. Wheat responded to CuONPs with increased release of DMA, citrate, and malate in the porewater and enhanced gluconate formation (Figure 3). The source of gluconate is unknown because wheat has not been reported to produce gluconate, but this metabolite is known to be secreted by bacteria and fungi (Wright et al. 2016). Wheat seeds are carriers of endophytes, which were not always eliminated by the surface sterilization processes used in these studies.

The secreted wheat phytosiderophore DMA, amino acids, and low–molecular weight organic acids will complex with Cu, removing free Cu from solution and driving the dissolution of the NPs forward. The solubility of CuO Ps without the plant exudates (the unplanted control) was limited (Figure 2B). Although doses >10 mg Cu/kg caused increased release of malate, citrate, and gluconate, DMA did not increase over the control until concentrations of the NPs were >30 mg Cu/kg. Wheat responds to Cu ions by increasing root exudates. Nian et al. (2002) observed enhanced root exudation of malate and citrate in wheat exposed to 40 μM (2540 μg/L) Cu ions, supplied as $CuCl_2$. Copper complexing root exudates increased in durum wheat on hydroponic exposure to 1 μM Cu^{2+} (Michaud et al. 2008). The concentration of free Cu^{2+} that induced exudation was 63 μg/L in the studies by Michaud et al. (2008), whereas in our studies the concentration range of Cu^{2+} was lower, from 0.32 to 3.6 μg/L. In our studies, whether the increased production of these metabolites was a direct metabolic response of the plant to root cell damage caused by the NPs and/or a consequence of enhanced soluble Cu awaits resolution.

Identification of chelation potential of metabolites in the porewaters

Geochemical modeling (MINTEQ) was employed to understand Cu chelation under equilibrium solution conditions for the <2-nm size fraction, the operationally defined dissolved fraction, in the porewater. In terms of complexation, Cu–citrate was predicted to be the dominant form of Cu in solution at CuONP doses of 100 mg Cu/kg or less (Figure 4). The role of citrate in the root exudates in Cu solubilization from the CuONPs is supported by observed enhanced dissolution, by up to 10-fold, irrespective of pH (Mudunkotuwa et al. 2012). The formation of the Cu–malate complex, predicted in significant amounts (Figure 4), particularly at CuONP doses of 10 and 30 mg Cu/kg sand, similarly should promote CuONP dissolution. Although the stability constant for Cu–malate ($\log K = 4.53$) is lower than for

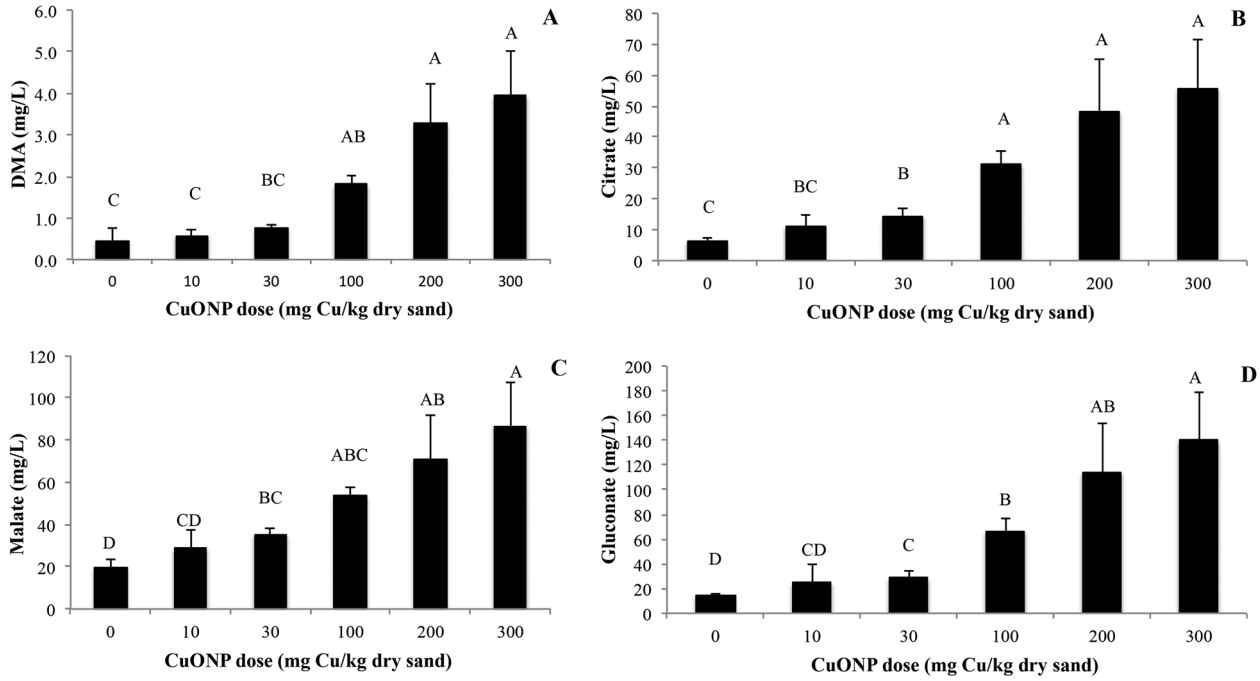

FIGURE 3: Effects of wheat growth with copper oxide nanoparticles (CuONP) on deoxymugineic acid (**A**), ($n = 3$) and the low–molecular weight organic acids, citrate (**B**), malate (**C**), and gluconate (**D**), ($n = 9$) detected in the porewater. Treatments with the same letters are not significantly different ($\alpha = 0.05$) by Tukey's honestly significant difference after log transformation. Error bars are 95% confidence interval to illustrate the spread in the data.

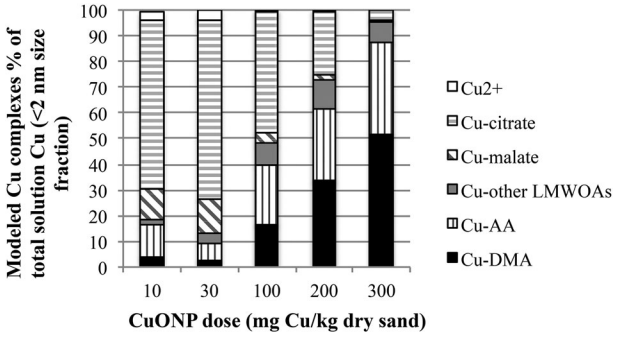

FIGURE 4: Copper (Cu) complexes in porewater at 10 d of wheat growth dosed with Cu oxide nanoparticles (CuONPs) as predicted by MINTEQ ($n = 3$). The MINTEQ model will precipitate any species above saturation. Model inputs included the ligands determined from chromatography of the porewater, soluble metals from 3-kDa ultrafiltrates with ICP-MS analysis (M < 2, defined as dissolved), and pH. Cu^{2+} = free copper ion; LMWOA = low–molecular weight organic acid; AA = amino acid; DMA = deoxymugineic acid.

citrate (log $K = 7.57$), for the 1:1 complexes there is sufficient concentration of malate to bind 12 to 14% of the soluble Cu at the low dosing of NPs, contributing to dissolution of the NPs. Complexation of Cu by amino acids in the root exudates was predicted to also be important as dose increased. The dominant Cu–amino acid complexes were Cu–arginine$^+$, Cu–glycine$^+$, Cu–(glycine)$_2$, and Cu–valine$^+$. At the high NP doses, 200 and 300 mg Cu/kg sand, complexing with DMA was important. Consequently, this modeling stresses different roles for the different metabolites in the root exudates in complexing Cu and, thus, promoting dissolution of the NPs.

Disturbed metal equilibrium in shoots caused by CuONP growth

In addition to increased Cu measure in shoots of plants grown with CuONPs, there were changes in other essential metals. Decrease in the other metals tested (Figure 5) in shoot and root tissue may result from the decrease in root surface area at high dosing of the NPs, limiting uptake. However, there are also specific plant–metal interactions that affect uptake.

Shoot Fe decreased at the highest dosing of CuONP (300 mg Cu/kg sand) compared to control plants (Figure 5A), coinciding with the highest DMA exudation and, thus, metal complexation potential (Figure 3A). Increases of Cu released from the NPs in the porewater (Figure 2B) may relate to formation of Cu–DMA complexes that impedes Fe uptake (Figure 4). The Cu–DMA complex could interrupt the Fe uptake mechanism of strategy II monocots, which uses predominantly Fe–DMA in wheat (Michaud et al. 2007; Ryan et al. 2013; Oburger et al. 2014). Application of ionic Cu was also antagonistic to Fe in hydroponic durum wheat (Michaud et al. 2008). In the present study with bread wheat, Fe in roots could not be accurately ascertained because of the Fe content of the sand grains adhering to the root surface—these grains could not be removed without potentially damaging the roots. The decrease in shoot Fe may also be attributed to the precipitation of Fe at the pH of this system, but geochemical modeling indicates that all solution phase Fe is complexed with gluconate. Manganese also decreased significantly in the shoots at CuONP doses of 100 mg Cu/kg sand and above compared with the control (Figure 5A and B). A similar observation was reported for cilantro shoots when CuONPs were added to potting soil

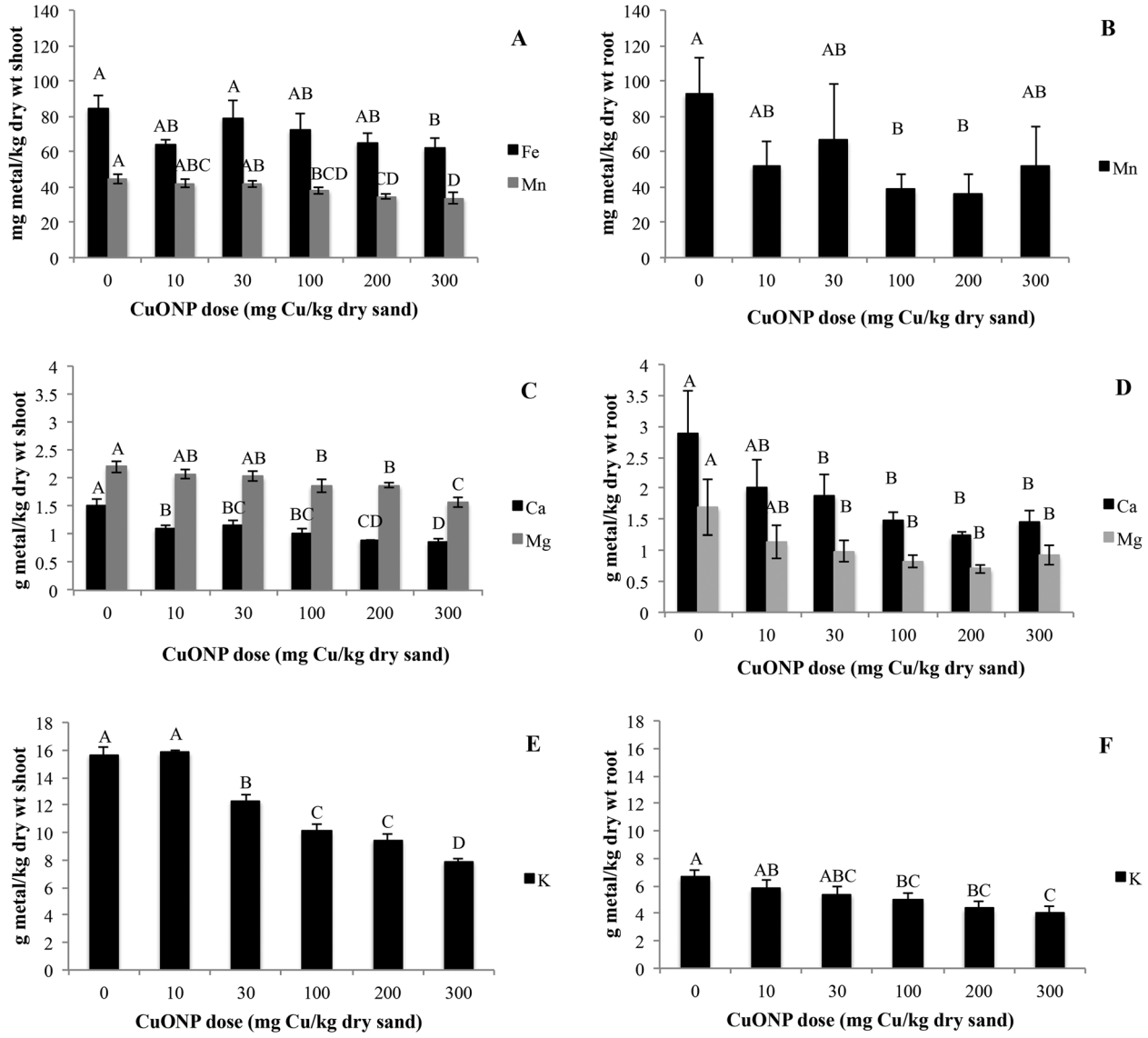

FIGURE 5: Metal accumulation in wheat plant at 10 d of growth with dosing of copper oxide nanoparticles (CuONPs): Fe and Mn shoots (**A**), Mn roots (**B**), Ca and Mg shoots (**C**), Ca and Mg roots (**D**), K shoots (**E**), and K roots (**F**), ($n = 9$). Treatments with the same letters are not significantly different ($\alpha = 0.05$) by Tukey's honestly significant difference after log transformation Error bars are 95% confidence interval to illustrate the spread in the data.

(Zuverza-Mena et al. 2015). In root tissue, Mn was less affected by growth with CuONPs (Figure 5B).

Calcium and Mg were dose-dependently lower in the shoot and root with CuONP exposure (Figure 5C and D). Both Mg and Ca are competing divalent cations taken up via nonselective channel. At 20 and 80 mg Cu/kg soil, CuONPs similarly depressed Ca and Mg in shoots of cilantro in potting mix soil (Zuverza-Mena et al. 2015). It is possible that Cu in solution from the CuONPs competed with Ca and Mg at the root surface, limiting their uptake. In hydroponically grown wheat, Mg and Ca ions reduced Cu ion toxicity (Luo et al. 2008; Wang et al. 2017).

A significant reduction in K in shoots and roots was found (Figure 5E and F), being more severe at higher NP dose. These results confirm previous findings with CuONPs for wheat (Dimkpa et al. 2012) and maize (Wang et al. 2012), as well as by exposure to Cu salts in chamomilla (Kováčik et al. 2012). Efflux of K^+ from plant cells is linked to increased oxidative stress (Murphy and Taiz 1997), a symptom of exposure of wheat roots to Cu^{2+} and CuONPs (Dimkpa et al. 2012; Adams et al. 2017).

Cu speciation and plant response

Of the several models that describe Cu toxicity in plants, the free ion activity model (FIAM) has toxicity driven by the activity of the free Cu ion. Differentiating toxicity attributable to NPs versus ions or Cu–organic matter complexes is a point of difficulty in defining the toxic effects of CuONPs (Ivask et al. 2014). In this section, the relationship between plant response (root and shoot length, root and shoot dry weight yield, and root and shoot tissue Cu concentration) and solution chemistries (Cu^{2+}, Cu complexes, pH, DOC, Ca, and Fe) is explored. The present study did not use growth conditions that maintained constant levels of soluble Cu or the concentration of exudates. Both increased with CuONP dosing (Figure 1), meaning that exudation and Cu

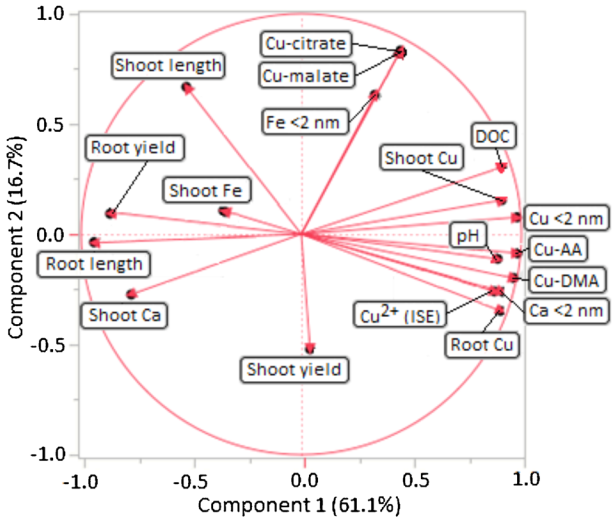

FIGURE 6: Principal component analysis of factors contributing to wheat plant uptake of Cu and the resulting bioresponse manifested as shoot and root length, shoot and root yield (dry wt basis), and shoot and root Cu concentration. Corresponding correlation matrix is in Table 1 and Supplemental Data, Table S6. AA = amino acid; Cu^{2+} (ISE) = free copper ions determined by ion-selective electrode; DMA = deoxymugineic acid.

dissolution were mutually promoting. Principal component analyses, therefore, were used to observe relationships among solution species and plant responses (Figure 6 and Table 1).

In the shoot tissue, Cu was correlated with all forms of Cu in solution (Figure 6 and Table 1). In the root tissue, Cu was likewise correlated with various forms of Cu in solution, with the exception of Cu–citrate and Cu–malate. The plants' response of shortened root and shoot length and decreased root dry weight correlated negatively DOC, Cu^{2+}, $Cu_{<2}$, Cu–DMA, and Cu–amino acid but not Cu–citrate or Cu–malate (Figure 6 and Table 1). In an experiment with Cu ion toxicity on wheat, Parker et al. (2001) demonstrated that Cu complexation by malonate, malate, and citrate in hydroponic systems decreased toxicity, although malate and malonate did not alleviate toxicity to the predicted extent; a portion of the Cu–malate and Cu–malonate was bioavailable contrary to the FIAM. Similarly, there is a lack of correlation between Cu–citrate or Cu–malate formed in the porewater during wheat growth and plant responses, indicating that these ligands were protective to wheat.

An increase in Cu–DMA formation during growth with CuONP at 100 mg Cu/kg (Figure 4) was associated with a threshold break with shoot accumulation >30 mg Cu/kg (Figure 1D). Copper–DMA formation was, therefore, correlated with increased Cu uptake and overthrow of plant protective mechanisms that otherwise limit Cu in the aboveground tissue. Puschenreiter et al. (2017) demonstrated increased DMA exudation in Fe-deficient soils and found enhanced Cu concentration in wheat shoots. Copper–phytosiderophores are likely taken up by oats (Ryan et al. 2013) and rice (Ando et al. 2013), but uptake is uncertain for barley (Ma and Nomoto 1993; Ma et al. 1993). Oats, rice, and barley, like wheat, are strategy II monocots, using phytosiderophores similar to DMA to chelate and take up Fe. In the wheat system, Fe–DMA was not predicted by geochemical modeling to form at any CuONP dose owing to the lower affinity of DMA for Fe than Cu (Murakami et al. 1989). With geochemical modeling, DMA is predicted to be 100% complexed with Cu over a pH range of 6 to 11; complexation of DMA with Cu and Fe is consistent over relevant environmental pH values. Thus, because there would be limited Fe–DMA complexation, reduced uptake of Fe would be expected with CuONP exposure. Similarly, in Fe-deficient soils, the presence of Cu and other metals limited the formation of Fe–DMA complexes and uptake of Fe into wheat (Puschenreiter et al. 2017). In the present study conditions for seed-grown young seedlings, low levels of CuONPs had little impact on Fe homeostasis (Figure 5A), meaning a dose <200 mg Cu/kg sand as CuONPs did not adversely affect Fe levels. The Fe shoot concentration was not correlated with other test variables (Supplemental Data, Tables S6 and S7). Copper concentration in shoots was negatively correlated with shoot concentrations of Ca, Mg, Mn, and K (Supplemental Data, Figure S2 and Table S7). These relationships display discrimination for uptake of these ions relative to Cu.

Modeling CuONP toxicity is still in its infancy; no model of NP uptake or direct toxicity yet exists, despite several studies showing that plant uptake of CuONPs occurs in hydroponics and soil for rice (Peng et al. 2015, 2017) and maize (Wang et al. 2012). Taken together, this may mean that Cu toxicity from CuONPs in these systems is derived from all forms, including the NPs (Mudunkotuwa et al. 2012), and certain bioavailable Cu complexes but with minor effects of free Cu^{2+} ions.

TABLE 1: Correlation matrix for factors in Figure 6

	Cu^{2+} (μg/L)	$Cu_{<2}$ (μg/L)	Cu-DMA (μg/L)	Cu-AA (μg/L)	Cu-citrate (μg/L)	Cu-malate (μg/L)	Cu shoot (mg/kg)	Cu root (mg/kg)	Root length (cm)	Shoot length (cm)	Root yield (g)	Shoot yield (g)
Cu shoot (mg/kg)	0.704[a]	0.895[a]	0.836[a]	0.875[a]	0.552[a]	0.489[a]	1.000[a]	0.828[a]	–0.850[a]	–0.295[b]	–0.697[a]	–0.139[b]
Cu root (mg/kg)	0.844[a]	0.836[a]	0.923[a]	0.900[a]	0.100[b]	0.086[b]	0.828[a]	1.000[a]	–0.846[a]	–0.627[a]	–0.830[a]	0.123[b]
Root length (cm)	–0.809[a]	–0.931[a]	–0.909[a]	–0.922[a]	–0.447[b]	–0.479[b]	–0.850[a]	–0.846[a]	1.000[a]	0.432[a]	0.812[a]	–0.061[b]
Shoot length (cm)	–0.651[a]	–0.503[a]	–0.669[a]	–0.609[a]	0.281[b]	0.311[b]	–0.295[b]	–0.627[a]	0.431[a]	1.000[a]	0.446[a]	–0.333[a]
Root yield (g)	–0.782[a]	–0.809[a]	–0.844[a]	–0.833[a]	–0.242[b]	–0.328[b]	–0.697[a]	–0.830[a]	0.812[a]	0.446[a]	1.000[a]	–0.091[a]
Shoot yield (g)	0.152[b]	0.038[b]	0.151[b]	0.094[b]	–0.322[b]	–0.233[b]	–0.139[b]	0.123[b]	–0.061[b]	–0.333[b]	–0.091[b]	1.000[a]

[a]Indicate correlation coefficients that are significant (α = 0.05). Correlation was estimated using row-wise comparisons.
[b]Indicate no significant relationships between those factors. Correlation was estimated using row-wise comparisons.
AA = amino acid; DMA = deoxymugineic acid.

Clearly, the specific exposure medium is highly influential in terms of CuONPs and their biogeochemistry (Wang et al. 2013), and the toxicity mechanisms of CuONPs remain inconclusive (Djurišić et al. 2015). For example, low-pH systems may drive toxicity purely from ion release from the CuONPs (Shi et al. 2011; Misra et al. 2012), whereas in higher-pH systems such as calcareous soils (pH >8), CuONP toxicity could be driven by CuONP uptake and dissolution of the NPs in the rhizosphere controlled by complexation. As NP dose increased, complexation was dominant (such as Cu–DMA or Cu–citrate) and toxicity increased. These findings implied that a greater understanding of the components of DOC released into the rhizosphere from plant roots is crucial in making a deterministic toxicity model to describe how CuONPs may be transformed and have bioavailability in agricultural settings. These processes are relevant in whole soil because root exudates are essential components for plants to obtain Fe and other micronutrients from insoluble minerals in complex soil environments.

CONCLUSION

Effects of CuONPs on wheat growth and uptake of Cu and other micronutrients involve complex processes occurring in the rhizosphere and in planta. Challenges to wheat roots with high concentrations (>100 mg Cu/kg sand) of CuONPs result in greater root exudation and enhanced Cu solubility, Cu uptake, and plant toxicity responses, observed as decreases in root length and biomass. The presence of soluble, bioavailable Cu complexes in the rhizosphere was correlated with this plant response.

Root exudation may serve as a defense mechanism against metal toxicity, but when challenged with higher dosing of CuONPs, these root exudates enhanced solubility of the NPs, overwhelming Cu tolerance in plants and breaking Cu homeostasis. The association of CuONPs at the wheat root surface may create toxicity as dissolution proceeds. The interplay between higher concentrations of NPs and increased root exudation, whether as a result of the NP or released ions, was found to drive dissolution through complexation. Damage to plant cell integrity may exacerbate this dissolution process in a feed-forward mechanism. The increased uptake of Cu into shoots with increasing CuONP dose coincided with lower levels of Ca, Mg, Mn, K, and Fe in the wheat shoots compared to controls. In particular, Fe uptake in this system may be at a competitive disadvantage as a result of conditions favoring Cu–DMA and possibly restricting or eliminating Fe–DMA complexation. These findings suggest possible problems in plant health as the wheat matures in the presence of CuONPs.

Supplemental Data—The Supplemental Data are available on the Wiley Online Library at DOI: 10.1002/etc.4226.

Acknowledgment—The present study was supported by a grant from the US Department of Agriculture (USDA-NIFA 10867118) and the Utah Water Research Laboratory (Utah Mineral Lease Funds).

Data Availability—Data, associated metadata, and calculations are available from the corresponding author (joan.mclean@usu.edu).

REFERENCES

Adams J, Wright M, Wagner H, Valiente J, Britt D, Anderson A. 2017. Cu from dissolution of CuO nanoparticles signals changes in root morphology. *Plant Physiol Biochem* 110:108–117.

Ahamed M, Alhadlaq H, Khan MAM, Karuppiah P, Al-Dhabi NA. 2013. Synthesis, characterization, and antimicrobial activity of copper oxide nanoparticles. *J Nanomater* 8:4467–4479.

Albalasmeh AA, Berhe AA, Ghezzehei TA. 2013. A new method for rapid determination of carbohydrate and total carbon concentrations using UV spectrophotometry. *Carbohydr Polym* 97:253–261.

American Public Health Association. 2012. *Standard Methods for the Examination of Water and Wastewater*, 22nd ed. Washington, DC.

Ando Y, Nagat S, Yanagisawa S, Yoneyama T. 2013. Copper in xylem and phloem saps from rice (Oryza sativa): The effect of moderate copper concentrations in the growth medium on the accumulation of five essential metals and a speciation analysis of copper-containing compounds. *Funct Plant Biol* 40:89–100.

Anjum NA, Adam V, Kizek R, Duart, AC, Pereira E, Iqbal M, Lukatkin AS, Ahmad I. 2015. Nanoscale copper in the soil–plant system—Toxicity and underlying potential mechanisms. *Environ Res* 138:306–325.

Atha DH, Wang H, Petersen EJ, Cleveland D, Holbrook RD, Jaruga P, Dizdaroglu M, Xing B, Nelson B. 2012. Copper oxide nanoparticle mediated DNA damage in terrestrial plant models. *Environ Sci Technol* 46:1819–1827.

Baker AJM. 1981. Accumulators and excluders—Strategies in the response of plants to heavy metals. *J Plant Nutr* 3:643–654.

Bechtold T, Burtscher E, Turcanu A. 2002. Ca^{2+}-Fe^{3+}-d-gluconate-complexes in alkaline solution. Complex stabilities and electrochemical properties. *Journal of the Chemical Society Dalton Transactions* 2002:2683–2688.

Bondarenko O, Ivask A, Käkine A, Kahru A. 2012. Sub-toxic effects of CuO nanoparticles on bacteria: Kinetics, role of Cu ions and possible mechanisms of action. *Environ Pollut* 169:81–89.

Callahan DL, Baker AJM, Kolev SD, Wedd AG. 2006. Metal ion ligands in hyperaccumulating plants. *J Biol Inorg Chem* 11:2–12.

Chen Y-T, Wang Y, Yeh K-C 2017. Role of root exudates in metal acquisition. *Curr Opin Plant Biol* 39:66–72.

Clemens S. 2001. Molecular mechanisms of plant metal tolerance and homeostasis. *Planta* 212:475–486.

Clemens S, Palmgren M, Krämer U. 2002. A long way ahead: Understanding and engineering plant metal accumulation. *Trends Plant Sci* 1385:309–315.

Cohen AC. 1959. Simplified estimators for the normal distribution when samples are singly censored or truncated. *Technometrics* 1:217–237.

Creager MS, Jenkins JE, Thagard-Yeaman LA, Brooks AE, Jones JA, Lewis RV, Holland GP, Yarger JL. 2010. Solid-state NMR comparison of various spiders' dragline silk fiber. *Biomacromolecules* 11:2039–2043.

David CA, Galceran J, Rey-Castro C, Puy J, Companys E, Salvador J, Monne J, Wallace R, Vakourov A. 2012. Dissolution kinetics and solubility of ZnO nanoparticles followed by AGNES. *J Phys Chem C* 116:11758–11767.

Davis RD, Beckett PHT. 1978. Upper critical levels of copper in young barley, wheat, rape, lettuce and ryegrass, and of nickel and zinc in young barley and ryegrass. *New Phytol* 80:23–32.

Dimkpa CO, Bindraban PS. 2017. Nanofertilizers: New products for the industry? *J Agric Food Chem* 66:6462–6473.

Dimkpa CO, Calder A, Britt DW, McLean JE, Anderson AJ. 2011. Response of soil bacterium, *Pseudomonas chlororaphis* O6 to comercial metal oxide nanoparticles compared with responses to metal ions. *Environ Pollut* 159:1749–1756.

Dimkpa CO, Latta DE, McLean JE, Britt DW, Boyanov MI, Anderson AJ. 2013. Fate of CuO and ZnO nano- and microparticles in the plant environment. *Environ Sci Technol* 47:4734–4742.

Dimkpa CO, McLean, JE, Britt DW, Anderson AJ. 2015. Nano-CuO and interaction with nano-ZnO or soil bacterium provide evidence for the

interference of nanoparticles in metal nutrition of plants. *Ecotoxicology* 24:119–129.

Dimkpa CO, McLean JE, Latta DE, Manangón E, Britt DW, Johnson WP, Boyanov MI, Anderson AJ. 2012. CuO and ZnO nanoparticles: Phytotoxicity, metal speciation, and induction of oxidative stress in sand-grown wheat. *J Nanopart Res* 14:1125.

Djurišić AB, Leung YH, Ng AMC, Xu XY, Lee PKH, Degger N, Wu RSS. 2015. Toxicity of metal oxide nanoparticles: Mechanisms, characterization, and avoiding experimental artefacts. *Small* 11:26–44.

Elmer WH, White JC. 2016. The use of metallic oxide nanoparticles to enhance growth of tomatoes and eggplants in disease infested soil or soilless medium. *Environ Sci Nano* 3:1072–1079.

Fageria NK. 2001. Adequate and toxic levels of copper and manganese in upland rice, common bean, corn, soybean, and wheat grown on an oxisol. *Commun Soil Sci Plant Anal* 32:1659–1676.

Gajda T, Gyurcsik B, Jakusch T, Burger K, Henry B, Delpuech J-J. 1998. Coordination chemistry of polyhydroxy acids: Role of the hydroxy groups. *Inorganica Chim Acta* 275–276:130–140.

Gajjar P, Pettee B, Britt DW, Huang W, Johnson WP, Anderson AJ. 2009. Antimicrobial activities of commercial nanoparticles against an environmental soil microbe, *Pseudomonas putida* KT2440. *J Biol Eng* 3:9.

Gao X, Avellan A, Laughton S, Vaidya R, Rodrigues SM, Casman EA, Lowry GV. 2018. CuO nanoparticle dissolution and toxicity to wheat (Triticum aestivum) in rhizosphere soil. *Environ Sci Technol* 52:2888–2897.

Gunawan C, Teoh WY, Marquis CP, Amal R. 2011. Cytotoxic origin of copper(II) oxide nanoparticles: Comparative studies with micron-sized particles, leachate, and metal salts. *ACS Nano* 5:7214–7225.

Guo L, Santschi PH. 2007. Ultrafiltration and its application to sampling and characterisation of aquatic colloids. In Wilkinson KJ, Lead JR, eds, *Environmental Colloids and Particles: Behaviour, Separation and Characterisation*, Vol 10. John Wiley & Sons, Hoboken, NJ, USA, pp 159–222.

Gustafsson JP. 2014. *Visual MINTEQ, A Windows Version of MINTEQA2*, Ver 3.1 [cited 2018 July 1]. Available from: vminteq.lwr.kth.se.

Hortin J. 2017. Behavior of copper oxide nanoparticles in soil pore waters as influenced by soil characteristics, bacteria, and wheat roots. MS Thesis. Utah State University, Logan, UT, USA. [cited 2018 July 1]. Available from: https://digitalcommons.usu.edu/etd/6895/.

Ivask A, Juganson K, Bondarenko O, Mortimer M, Aruoja V, Kasemets K, Blinova I, Heinlaan M, Slaveykova V, Kahru A. 2014. Mechanisms of toxic action of Ag, ZnO and CuO nanoparticles to selected ecotoxicological test organisms and mammalian cells in vitro: A comparative review. *Nanotoxicology* 8(Suppl. 1):57–71.

Jones DL. 1998. Organic acids in the rhizosphere—A critical review. *Plant Soil* 205:25–44.

Jones J, Case V. 1990. Sampling, handling, and analyzing plant tissue samples. In Westerman RL, ed, *Soil Testing and Plant Analysis*. American Society of Agronomy, Madison, WI, pp 389–427.

Joshi S, Ghosh I, Pokhrel S, Mädler L, Nau WM. 2012. Interactions of amino acids and polypeptides with metal oxide nanoparticles probed by fluorescent indicator adsorption and displacement. *ACS Nano* 6:5668–5679.

Keller AA, McFerran S, Lazareva A, Suh S. 2013. Global life cycle releases of engineered nanomaterials. *J Nanopart Res* 15:1692.

Kim S, Lim H, Lee I. 2010. Enhanced heavy metal phytoextraction by *Echinochloa crus-galli* using root exudates. *J Biosci Bioeng* 109:47–50.

Kopittke PM, Blamey FPC, McKenna BA, Wang P, Menzies NW. 2011. Toxicity of metals to roots of cowpea in relation to their binding strength. *Environ Toxicol Chem* 30:1827–1833.

Kopittke PM, Menzies NW, Wang P, McKenna BA, Wehy JB, Lombi E, Kinraide TB, Blamey FPC. 2014. The rhizotoxicity of metal cations is related to their strength of binding to hard ligands. *Environ Toxicol Chem* 33:268–277.

Kováčik J, Klejdus B, Hedbavny J, Stork F, Grúz J. 2012. Modulation of copper uptake and toxicity by abiotic stresses in *Matricaria chamomilla* plants. *J Agric Food Chem* 60:6755–6763.

Lee J, Mahendra S, Alvarez PJJ. 2010. Potential environmental and human health impacts of nanomaterials used in the construction industry. *ACS Nano* 4:3580–3590.

Lee W-M, An Y-J, Yoon H, Kweon H-S. 2008. Toxicity and bioavailability of copper nanoparticles to the terrestrial plants mung bean (*Phaseolus radiatus*) and wheat (*Triticum aestivum*): Plant agar test for water-insoluble nanoparticles. *Environ Toxicol Chem* 27:1915–1921.

Lindsay WL. 1979. *Chemical Equilibria in Soils*. John Wiley and Sons, New York, NY, USA.

Luo X, Li L, Zhou D. 2008. Effect of cations on copper toxicity to wheat root: Implications for the biotic ligand model. *Chemosphere* 73:401–406.

Lynch I, Dawson KA. 2008. Protein-nanoparticle interactions. *Nano Today* 3:40–47.

Ma JF, Kusanoa G, Kimuraa S, Nomoto K. 1993. Specific recognition of mugineic acid-ferric complex by barley roots. *Phytochemistry* 34: 599–603.

Ma JF, Nomoto K. 1993. Inhibition of mugineic acid-ferric complex uptake in barley by copper, zinc and cobalt. *Physiol Plant* 89:331–334.

Marschner H. 1995. *Mineral Nutrition of Higher Plants*, 3rd ed. Academic, San Diego, CA, USA.

McLean JE, Pabst MW, Miller CD, Dimkpa CO, Anderson AJ. 2013. Effect of complexing ligands on the surface adsorption, internalization, and bioresponse of copper and cadmium in a soil bacterium, *Pseudomonas putida*. *Chemosphere* 91:374–382.

Meychik N, Nikolaeva Y, Kushunina M, Yermakov I. 2016. Contribution of apoplast to short-term copper uptake by wheat and mung bean roots. *Funct Plant Biol* 43:403–412.

Michaud AM, Bravin MN, Galleguillos M, Hinsinger P. 2007. Copper uptake and phytotoxicity as assessed in situ for durum wheat (*Triticum turgidum durum* L.) cultivated in Cu-contaminated, former vineyard soils. *Plant Soil* 298:99–111.

Michaud AM, Chappellaz C, Hinsinger P. 2008. Copper phytotoxicity affects root elongation and iron nutrition in durum wheat (*Triticum turgidum durum* L.). *Plant Soil* 310:151–165.

Misra SK, Dybowska A, Berhanu D, Luoma SN, Valsami-Jones E. 2012. The complexity of nanoparticle dissolution and its importance in nanotoxicological studies. *Sci Total Environ* 438:225–232.

Monreal M, DeRosa M, Mallubhotla SC, Bindraban PS, Dimkpa C. 2015. Nanotechnologies for increasing the crop use efficiency of fertilizer-micronutrients. *Biol Fertil Soils* 52:423–437.

Mudunkotuwa IA, Pettibone JM, Grassian VH. 2012. Environmental implications of nanoparticle aging in the processing and fate of copper-based nanomaterials. *Environ Sci Technol* 46:7001–7010.

Murakami T, Ise K, Hayakawa M, Kamei S, Takagi S. 1989. Stabilities of metal complexes of mugineic acids and their specific affinities for iron(III). *Chem Lett* 12:2137–2140.

Murphy A, Taiz L. 1997. Correlation between potassium efflux and copper sensitivity in 10 *Arabidopsis* ecotypes. *New Phytol* 136:211–222.

Nian H, Yang ZM, Ahn SJ, Cheng ZJ, Matsumoto H. 2002. A comparative study on the aluminium- and copper-induced organic acid exudation from wheat roots. *Physiol Plant* 116:328–335.

Oburger E, Gruber B, Schindlegger Y, Schenkeveld WDC, Hann S, Kraemer SM, Wenzel WW, Puschenreiter M. 2014. Root exudation of phytosiderophores from soil-grown wheat. *New Phytol* 203: 1161–1174.

Parker DR, Norvell WA, Chaney RL. 1995. GEOCHEM-PC: A chemical speciation program for IBM and compatible personal computers. In Loeppert RH, Schwab AP, Goldberg S, eds, *Chemical Equilibrium and Reaction Models*. SSSA Special Publication 42. Soil Science Society of America, Madison, WI, pp 253–269.

Parker DR, Pedler JF, Ahnstrom ZAS, Resketo M. 2001. Reevaluating the free-ion activity model of trace metal toxicity toward higher plants: Experimental evidence with copper and zinc. *Environ Toxicol Chem* 20:899–906.

Peng C, Xu C, Liu Q, Sun L, Luo Y, Shi J. 2017. Fate and transformation of CuO nanoparticles in the soil-rice system during the life cycle of rice plants. *Environ Sci Technol* 51:4907–4917.

Peng C, Zhang H, Fang H, Xu C, Huang H, Wang Y, Sun L, Yuan X, Chen Y, Shi J. 2015. Natural organic matter-induced alleviation of the phytotoxicity to rice (*Oryza sativa* L.) caused by copper oxide nanoparticles. *Environ Toxicol Chem* 34:1996–2003.

Puschenreiter M, Gruber B, Wenzel WW, Schindlegger Y, Hann S, Spangl B, Schenkeveld WDC, Kreemer SM. 2017. Phytosiderophore-induced mobilization and uptake of Cd, Cu, Fe, Ni, Pb and Zn by wheat plants grown on metal-enriched soils. *Environ Exp Bot* 138:67–76.

Rachou J, Gagnon C, Sauvé S. 2007. Use of an ion-selective electrode for free copper measurements in low salinity and low ionic strength matrices. *Environ Chem* 4:90–97.

Rawat S, Pullagurala VLR, Hernandez-Molina M, Sun Y, Niu G, Hernandez-Viezcas JA, Peralta-Videa JR, Gardea-Torresdey JL. 2018. Impact of copper oxide nanoparticles on bell pepper (*Capsicum annum* L.) plants: A full life cycle study. *Environ Sci Nano* 5:83–95.

Reed S, Martens D. 1996. *Copper and zinc. In Sparks DL, ed, Methods of Soil Analysis. Part 3—Chemical Methods. SSSA Book Series*. Soil Science Society of America, Madison, WI, 703–722.

Rivera Gil P, Oberdörster G, Elder A, Puntes V, Parak WJ. 2010. Correlating physico-chemical with toxicological properties of nanoparticles: The present and the future. *ACS Nano* 4:5527–5531.

Rodrigues SM, Demokritou P, Dokoozlian N, Hendren CO, Karn B, Mauter MS, Sadik OA, Safarpour M, Unrine JM, Viers J, Welle P, Ehite JC, Wiesner MR, Lowry GV. 2017. Nanotechnology for sustainable food production: Promising opportunities and scientific challenges. *Environ Sci Nano* 4:767–781.

Ryan BM, Kirby JK, Degryse F, Harris H, Mclaughlin MJ, Cheiderich K. 2013. Copper speciation and isotopic fractionation in plants: Uptake and translocation mechanisms. *New Phytol* 199:367–378.

Sauve S, Hendershot W, Allen HE. 2000. Solid-solution partitioning of metals in contaminated soils: Dependence on pH, total metal burden, and organic matter. *Environ Sci Technol* 34:1125–1131.

Saxton KE, Rawls WJ. 2006. Soil water characteristic estimates by texture and organic matter for hydrologic solutions. *Soil Sci Soc Am J* 70:1569–1578.

Schindlegger Y, Oburger E, Gruber B, Schenkeveld WDC, Kraemer SM, Puschenreiter M, Koellensperger G, Hann S. 2014. Accurate LC-ESI-MS/MS quantification of 2′-deoxymugineic acid in soil and root related samples employing porous graphitic carbon as stationary phase and a $^{13}C_4$-labeled internal standard. *Electrophores* 35:1375–1385.

Shi J, Abid AD, Kennedy IM, Hristova KR, Silk WK. 2011. To duckweeds (*Landoltia punctata*), nanoparticulate copper oxide is more inhibitory than the soluble copper in the bulk solution. *Environ Pollut* 159:1277–1282.

Stampoulis D, Sinha SK, White JC. 2009. Assay-dependent phytotoxicity of nanoparticles to plants. *Environ Sci Technol* 43:9473–9479.

Stewart J, Hansen T, McLean JE, McManus P, Das D, Britt DW, Andereson AJ, Dimkpa CO. 2015. Salts affect the interaction of ZnO and CuO nanoparticles with wheat. *Environ Toxicol Chem* 34:2116–2125.

Trujillo-Reyes J, Majumdar S, Botez CE, Peralta-Videa JR, Gardea-Torresdey JL. 2014. Exposure studies of core-shell Fe/Fe_3O_4 and Cu/CuO NPs to lettuce (*Lactuca sativa*) plants: Are they a potential physiological and nutritional hazard? *J Hazard Mater* 267:255–263.

US Environmental Protection Agency. 1986 (and updates). Test methods for evaluating solid waste: Physical/chemical methods. SW-846. Washington, DC.

Violante A, Caporale AG. 2015. Biogeochemical processes at soil-root interface. *J Soil Sci Plant Nutr* 15:422–448.

Wang X, Ji D, Chen X, Ma Y, Yang J, Ma J, Li X. 2017. Extended biotic ligand model for predicting combined Cu-Zn toxicity to wheat (*Triticum aestivum* L.): Incorporating the effects of concentration ratio, major cations and pH. *Environ Pollut* 230:210–217.

Wang Z, Von Dem Bussche A, Kabadi PK, Kane AB, Hurt RH. 2013. Biological and environmental transformations of copper-based nanomaterials. *ACS Nano* 7:8715–8727.

Wang Z, Xie, X, Zhao J, Liu X, Feng W, White JC, Xing B. 2012. Xylem- and phloem-based transport of CuO nanoparticles in maize (*Zea mays* L.). *Environ Sci Technol* 46:4434–4441.

Wright M, Adams J, Yang K, McManus P, Jacobson J, Gade A, McLean J, Britt D, Anderson A. 2016. A root-colonizing pseudomonad lessens stress responses in wheat imposed by CuO nanoparticles. *PLoS One* 11(10): e0164635.

Xu M, Li J, Iwai H, Mei Q, Fujita D, Su H, Chen H, Hanagata N. 2012. Formation of nano-bio-complex as nanomaterials dispersed in a biological solution for understanding nanobiological interactions. *Sci Rep* 2:406. DOI: 10.1038/srep00406

Xuan Y, Scheuermann EB, Meda AR, Hayen H, von Wirén N, Weber G. 2006. Separation and identification of phytosiderophores and their metal complexes in plants by zwitterionic hydrophilic interaction liquid chromatography coupled to electrospray ionization mass spectrometry. *J Chromatogr A* 1136:73–81.

Yang K-Y, Doxey S, McLean JE, Britt WJ, Watson A, Al Qassy D, Jacobson AR, Anderson AJ. 2018. Remodeling of root morphology by CuO and ZnO nanoparticles by a beneficial pseudomonad. *Botany* 96:175–186.

Zuverza-Mena N, Medina-Velo IA, Barrio AC, Tan W, Peralta-Videa JR, Gardea-Torresdey JL. 2015. Copper nanoparticles/compounds impact agronomic and physiological parameters in cilantro (*Coriandrum sativum*). *Environ Sci* 17:1783–1793.

